Pergamon

Int. J. Heat Mass Transfer. Vol. 39, No. 6, pp. 1157–1164, 1996

0017-9310/96 $15.00 + 0.00

0017–9310(95)00213–8

Non-Darcy mixed convection along nonisothermal vertical surfaces in porous media

CHIEN-HSIN CHEN

Department of Mechanical Design Engineering, National Yunlin Polytechnic Institute, Yunlin 632, Taiwan, Republic of China

T. S. CHEN

Department of Mechanical and Aerospace Engineering and Engineering Mechanics, University of Missouri-Rolla, Rolla, MO 65401, U.S.A.

and

CHA'O-KUANG CHEN

Department of Mechanical Engineering, National Cheng Kung University, Tainan 701, Taiwan, Republic of China

(*Received* 3 *November* 1994 *and in final form* 12 *June* 1995)

Abstract—An analysis is performed for mixed convective flow through a fluid-saturated porous medium adjacent to a vertical surface with the heating condition of power-law variation in the wall temperature. The entire mixed convection regime is covered by the single parameter $\chi = [1+(Ra_x/Pe_x)^{0.5}]^{-1}$ from the pure forced convection limit ($\chi = 1$) to the pure free convection limit ($\chi = 0$). In modeling the flow through porous media, non-Darcy effects such as high-flow-rate inertia forces, no-slip boundary condition, near-wall porosity variation and thermal dispersion are taken into consideration. Because of the porosity variation in the near wall region, the stagnant thermal conductivity also varies accordingly. The aims of the present work are to examine the effects of non-Darcian flow phenomena on mixed convective transport and to demonstrate the variation in heat transfer predictions based on different flow models. A finite-difference scheme was used to solve the transformed system of equations. Numerical results show that non-Darcian and thermal dispersion effects have significant influences on velocity profiles, temperature profiles and heat transfer rates from the vertical surface.

INTRODUCTION

Transport processes through porous media play important roles in diverse applications, such as in geothermal operations, petroleum industries, thermal insulation, design of solid–matrix heat exchangers, chemical catalytic reactors, and many others. The study of convective heat transfer and fluid flow in porous media has received great attention in recent years. Most of the earlier studies [1–4] were based on Darcy's law which states that the volume-averaged velocity is proportional to the pressure gradient. The Darcy model is shown to be valid under the conditions of low velocities and small porosity [5]. In many practical situations the porous medium is bounded by an impermeable wall, has higher flow rates, and reveals nonuniform porosity distribution in the near wall region, making the Darcy's law inapplicable. To model the real physical situation better, it is therefore necessary to include the aforementioned non-Darcian terms in the analysis of convective transport in a porous medium. Thus, the present study focuses on the importance of non-Darcian effects on fluid flow and heat transfer through porous media.

The inertia effect is expected to be important at a higher flow rate and it can be accounted for through the addition of a velocity-squared term in the momentum equation, which is known as the Forchheimer's extension. The boundary effect may become significant when heat transfer is considered in a region very close to a solid boundary. The Brinkman's extension, which incorporates a viscous shear stress term into the momentum equation, together with the no-slip boundary condition, is usually used to shed light on the importance of boundary effects. The simultaneous effects of fluid inertia force and boundary viscous resistance upon flow and heat transfer in a constant-porosity porous medium were analyzed by Vafai and Tien [6] for forced convection and by Ranganathan and Viskanta [7] for mixed convection. From their reports, it was found that both boundary and inertia effects exhibit a significant influence on velocity distribution and heat transfer, especially for flows with a larger Reynolds number based on pore

NOMENCLATURE

C	inertia coefficient
Da_d	Darcy number based on particle diameter, K_∞/a^2
Da_x	local Darcy number, K_∞/x^2
D_t	empirical constant defined in equation (11)
d	particle diameter
Fo	Forchheimer number, $(K_\infty C_\infty/d)(\alpha_f/\nu)$
f	dimensionless stream function
g	gravitational constant
h	local heat transfer coefficient
K	permeability
k_d	stagnant thermal conductivity
k_e	effective thermal conductivity
k_f	thermal conductivity of fluid
k_s	thermal conductivity of particles
k_t	thermal dispersion conductivity
N	empirical constant in equation (6)
Nu_x	local Nusselt number, hx/k_e
P	pressure
Pe_d	Peclet number based on particle diameter
Pe_x	local Peclet number, $u_\infty x/\alpha_f$
Pr	Prandtl number of the fluid
q_w	local surface heat flux
Ra_x	local Rayleigh number, $g\beta(T_w-T_\infty)K_\infty x/\nu\alpha_f$
Ra_d	Rayleigh number based on particle diameter
T	temperature
u	x-component velocity
v	y-component velocity
x	streamwise coordinate
y	cross-stream coordinate.

Greek symbols

α_e	effective thermal diffusivity of the porous medium
α_f	thermal diffusivity of fluid
β	thermal expansion coefficient
η	pseudo-similarity variable
θ	dimensionless temperature
μ	dynamic viscosity
ν	kinematic viscosity
ξ	boundary effect parameter, $Da_d/(x/d)$
ρ	density of the fluid
σ	α_e/α_f
ϕ	porosity
τ_w	local wall shear stress
χ	nonsimilarity parameter
ψ	stream function.

Subscripts

∞	quantities away from the wall
w	quantities at the wall.

size, and thus these effects cannot be ignored. Also, detailed accounts of non-Darcy effects on natural convection in a porous cavity have been recently reported in Lauriat and Prasad [8, 9]. More recently, Choi and Kulacki [10] have investigated the effects of Brinkman and Forchheimer terms on mixed convection in a vertical annulus. In some applications, such as chemical catalytic reactors and packed-sphere beds, the porosity of the porous medium can no longer be deemed a constant. Owing to the variation in packing next to the solid wall, the measurements of Benenati and Brosilow [11] demonstrated a distinct porosity variation with a high-porosity region in the vicinity of the solid boundary. This nonuniform porosity distribution leads to the occurrence of a maximum velocity within the high-porosity region, which is recognized as the flow-channeling phenomenon [12, 13]. In studying the near-wall porosity variation, a simple exponential function is usually employed to approximate the porosity decay from the solid wall (see, for example [12–14]). In addition, the effects of transverse thermal dispersion are expected to be more noticeable when inertia effects are prevalent, as reported by Cheng [15] and Plumb [16]. This dispersive transport results from the mixing of local fluid streams as the fluid moves past the solid particles.

Many previous reports are restricted to situations in which similarity solutions exist [1–3]. However, the flow and thermal fields in mixed convection from surfaces in porous media are nonsimilar in nature. Nonsimilarity solutions for nonsimilar natural and mixed convection problems are reported by using the local similarity and nonsimilarity methods [17, 18]. Solutions from these methods are approximate due to the neglect of higher order terms in the governing equations. A more accurate solution for nonsimilar boundary layer flows can be obtained by using a finite-difference scheme [19], which was employed recently by Aldoss *et al.* [20] and Hsieh *et al.* [21] to solve the problems of mixed convection along nonisothermal horizontal and vertical surfaces within Darcy porous media. However, the non-Darcian flow phenomena often involved in porous media are neglected in their analyses.

The objective of the present work is to investigate numerically the influence of non-Darcian terms on mixed convection heat transfer along a vertical surface embedded in a porous medium, under the condition of variable wall temperature in the form $T_w(x) = T_\infty + ax^n$. A single nonsimilarity parameter $\chi = [1+(Ra_x/Pe_x)^{0.5}]^{-1}$, which varies from one for pure forced convection to zero for pure free convec-

tion, is introduced to cover the entire mixed convection regime. The Darcy–Forchheimer–Brinkman flow model [6], with a variable porosity distribution, is employed to represent momentum transport of the convective fluid. The variation of porosity in the vicinity of the solid boundary is approximated by an exponential function. In addition, the effects of transverse thermal dispersion are included in the energy equation, along with a variable stagnant conductivity. Numerical solutions for the governing differential equations are generated by an efficient finite-difference algorithm. The importance of the non-Darcian terms will be illustrated by comparing results based on the non-Darcy model with those of a Darcy flow. Results of major interest, such as temperature profiles, velocity profiles, and the local Nusselt number, are presented for some representative exponential values of the power-law wall temperature variation.

ANALYSIS

Consider the problem of mixed convection along an impermeable vertical plate embedded in a fluid-saturated porous medium. The vertical plate is assumed to be heated in such a way that its surface temperature varies in the power-law form, $T_w(x) = T_\infty + ax^n$, where a is a constant and n is the exponent. The streamwise coordinate is denoted by x, and that normal to it is denoted by y. The gravitational acceleration g is acting downward in the direction opposite to the x coordinate. In the formulation of the present problem the following common assumptions are made: the flow is steady, incompressible and two-dimensional (2D); and the convective fluid and the porous matrix are everywhere in local thermodynamic equilibrium. Under these assumptions and the application of the Boussinesq and boundary-layer approximations, the governing conservation equations, with momentum equation based on the Darcy–Forchheimer–Brinkman model, can be written as [6]

$$\frac{\partial u}{\partial x} + \frac{\partial v}{\partial y} = 0 \tag{1}$$

$$\frac{\mu}{K}u + \rho C u^2 = -\frac{\partial P}{\partial x} + \frac{\mu}{\phi}\frac{\partial^2 u}{\partial y^2} + \rho g \beta (T - T_\infty) \tag{2}$$

$$u\frac{\partial T}{\partial x} + v\frac{\partial T}{\partial y} = \frac{\partial}{\partial y}\left(\alpha_e \frac{\partial T}{\partial y}\right). \tag{3}$$

In the above equations, u and v are the velocity components along the x and y directions; T and P are the temperature and pressure; ρ, μ and β are the density, dynamic viscosity and thermal expansion coefficient of the fluid; K, C and ϕ are the permeability, inertia force parameter and porosity of the porous medium; and $\alpha_e = k_e/(\rho c)$ is the effective thermal diffusivity of the porous medium, with k_e denoting the effective thermal conductivity of the saturated porous medium and ρc the product of the density and specific heat of the fluid. The second term on the left-hand side of the momentum equation, equation (2), accounts for an additional pressure loss due to the fluid inertia force, while the second term on its right-hand side represents the viscous shear force in the boundary layer. The appropriate boundary conditions for the problem are

$$u = v = 0 \quad T = T_w(x) = T_\infty + ax^n \quad \text{at} \quad y = 0 \tag{4}$$

$$u \to u_\infty \quad T \to T_\infty \quad \text{as} \quad y \to \infty. \tag{5}$$

It is noted that $n = 0$ corresponds to the case of an isothermal plate.

In order to examine the nonuniform porosity effects, an exponential decrease is presumed to account for the functional dependence of porosity on the distance y from the wall, as was used in several published reports [12–14]:

$$\phi = \phi_\infty + (\phi_w - \phi_\infty)\exp(-Ny/d) \tag{6}$$

where ϕ_∞ is the free-stream porosity, ϕ_w is the porosity at wall, and N is an experimental parameter which depends on the packing of particles next to the solid wall. Measurements show that the porosity of a packed-sphere bed decreases from a value of 0.8–1.0 at the wall to 0.36–0.4 in the bulk of the bed [11, 22]. The porosity oscillates around the free-stream value with the oscillations damped out at about 4.5–5 particle diameters from the wall. The constants ϕ_∞ and ϕ_w chosen in a recent paper [23] are $\phi_\infty = 0.4$, $\phi_w = 0.9$. A sharp exponential decrease, $N = 6$, is used to reflect the rapid porosity change near the wall [24]. Note that the oscillations of porosity, which are considered to be secondary, are neglected in the present analysis. Both permeability K and inertia coefficient C of the porous matrix depend on the porosity and particle diameter and can be determined from the widely-known correlations proposed by Ergun [25]

$$K = \frac{d^2\phi^3}{150(1-\phi)^2} \tag{7}$$

$$C = \frac{1.75(1-\phi)}{d\phi^3} \tag{8}$$

where d is the particle diameter. It can be seen that the permeability and inertia coefficient will vary with porosity decay from the wall.

Thermal dispersion effects are anticipated to be significant when inertia effects are prevalent. It is well known that the effective thermal conductivity k_e of a saturated porous medium can be expressed as a sum of the stagnant thermal conductivity k_d (due to molecular diffusion) and the thermal dispersion conductivity k_t (due to mechanical dissipation); in other words,

$$k_e = k_d + k_t. \tag{9}$$

The stagnant thermal conductivity of the porous medium can be computed from the following semi-analytical expression [26]

$$\frac{k_d}{k_f} = [1-\sqrt{(1-\phi)}] + \frac{2\sqrt{(1-\phi)}}{1-\lambda B} \times \left[\frac{(1-\lambda)B}{(1-\lambda B)^2}\ln\left(\frac{1}{\lambda B}\right) - \frac{B+1}{2} - \frac{B-1}{1-\lambda B}\right] \quad (10)$$

where $B = 1.25[(1-\phi)/\phi]^{10/9}$ and $\lambda = k_f/k_s$ is the ratio of the thermal conductivity of fluid phase to that of solid phase. Equation (10) reveals that the stagnant thermal conductivity is a function of position for a nonuniform porosity medium. As proposed by Hsu and Cheng [27], the thermal dispersion conductivity can be given in the form

$$\frac{k_t}{k_f} = D_t \frac{1-\phi}{\phi^2}\frac{ud}{\alpha_f} \quad (11)$$

where D_t is an empirical contant and α_f is the thermal diffusivity of the fluid.

To facilitate the present analysis, the system of equations (2)–(5) will be transformed into a dimensionless form by introducing

$$\eta = \frac{y}{x}Pe_x^{0.5}\chi^{-1} \quad \chi = [1+(Ra_x/Pe_x)^{0.5}]^{-1} \quad (12)$$

$$f(\chi,\eta) = \psi(x,y)\chi/(\alpha_f Pe_x^{0.5})$$

$$\theta = (T-T_\infty)/(T_w-T_\infty) \quad (13)$$

where the stream function ψ satisfies the continuity equation, equation (1), with $u = \partial\psi/\partial y$ and $v = -\partial\psi/\partial x$; $Pe_x = u_\infty x/\alpha_f$ is the local Peclet number; $Ra_x = g\beta(T_w-T_\infty)K_\infty x/\nu\alpha_f$ is the local Rayleigh number; and χ is the nonsimilarity mixed convection parameter.

Substituting equations (12) and (13) into equations (2)–(5), we have the following set of non-dimensional equations:

$$\frac{\xi(x)}{\phi}\left[Pe_d^{0.5} + Ra_d^{0.5}\left(\frac{x}{d}\right)^{0.5n}\right]^2\frac{\partial^3 f}{\partial\eta^3} - Fo\left[Pe_d^{0.5} + Ra_d^{0.5}\left(\frac{x}{d}\right)^{0.5n}\right]^2\left(\frac{C}{C_\infty}\right)\left(\frac{\partial f}{\partial\eta}\right)^2 - \left(\frac{K_\infty}{K}\right)\frac{\partial f}{\partial\eta} + (1+FoPe_d)\chi^2 + (1-\chi)^2\theta = 0 \quad (14)$$

$$\sigma\frac{\partial^2\theta}{\partial\eta^2} + \left\{\tfrac{1}{2}[1+n(1-\chi)]f + \frac{\partial\sigma}{\partial\eta}\right\}\frac{\partial\theta}{\partial\eta} - n\frac{\partial f}{\partial\eta}\theta = \frac{n}{2}\chi(1-\chi)\left(\frac{\partial\theta}{\partial\eta}\frac{\partial f}{\partial\chi} - \frac{\partial f}{\partial\eta}\frac{\partial\theta}{\partial\chi}\right) \quad (15)$$

$$\frac{\partial f}{\partial\eta}(\chi,0) = 0$$

$$[1+n(1-\chi)]f(\chi,0) - n\chi(1-\chi)\frac{\partial f}{\partial\chi}(\chi,0) = 0$$

$$\theta(\chi,0) = 1 \quad (16)$$

$$\frac{\partial f}{\partial\eta}(\chi,\infty) = \chi^2, \quad \theta(\chi,\infty) = 0 \quad (17)$$

where $Fo = (K_\infty C_\infty/d)(\alpha_f/\nu)$ is the Forchheimer number; $\xi(x) = Da_d/(x/d)$ is the boundary effect parameter with $Da_d = K_\infty/d^2$; $Pe_d = u_\infty d/\alpha_f$ and $Ra_d = Ra_x|_{x=d} = g\beta(ad^n)K_\infty d/\nu\alpha_f$ are respectively the Peclet number and Rayleigh number based on particle diameter; $\sigma = \alpha_e/\alpha_f$ and K_∞ and C_∞ are the permeability and inertia coefficient in the bulk region.

The physical quantities of major interest are the velocity components u and v, the wall shear stress $\tau_w(x)$ and the local heat flux $q_w(x)$. Using the dimensionless variables in equations (12) and (13), u and v become

$$u = u_\infty\chi^{-2}f \quad (18)$$

$$v = -u_\infty Pe_x^{-0.5}\chi^{-1}\left\{\tfrac{1}{2}[1+n(1-\chi)]f - \tfrac{1}{2}[1-n(1-\chi)]\eta f' - \frac{n}{2}\chi(1-\chi)\frac{\partial f}{\partial\chi}\right\}. \quad (19)$$

The local wall shear stress is defined as $\tau_w(x) = \mu(\partial u/\partial y)_{y=0}$, and can be cast into a dimensionless form as

$$\tau_w(x^2/\mu\alpha_f)(Pe_x^{0.5} + Ra_x^{0.5})^{-3} = f''(\chi,0). \quad (20)$$

The most important result to be determined is the heat transfer rate from the vertical plate. Consider first the local heat flux along the vertical surface, which can be computed from $q_w(x) = -k_e(\partial T/\partial y)_{y=0}$. Results for local heat transfer rates from the surface of the vertical plate are usually represented in terms of the local Nusselt number $Nu_x = hx/k_e$, where $h(x) = q_w(x)/[T_w(x)-T_\infty]$ is the local heat transfer coefficient. The local Nusselt number in terms of the new variables is

$$Nu_x(Pe_x^{0.5} + Ra_x^{0.5})^{-1} = -\theta'(\chi,0) \quad (21)$$

The primes in equations (18)–(21) denote partial differentiations with respect to η.

Numerical solutions to equations (14)–(17) were obtained on the basis of an efficient finite-difference scheme as described by Cebeci and Bradshaw [19]. This numerical scheme has several very desirable features that make it appropriate for the solution of parabolic partial differential equations. These features include a second-order accuracy with arbitrary χ and η spacings, allowing very rapid χ variations, and allowing easy programming of the solution of a large number of coupled equations. In the interest of brevity, the details of the solution procedure by this method are not repeated here.

RESULTS AND DISCUSSION

The influence of various non-Darcian flow phenomena on mixed convection along a nonisothermal vertical plate in a porous medium is examined and dis-

cussed in this section. Following the arguments outlined in the previous reports [2, 21], the range of the exponent n for which the present problem is physically realistic is $0 \leqslant n \leqslant 1$. Numerical results were obtained for values of n within the above range and for the following values of physical quantities: water at $Pr = 6.95$, $u_\infty = 0.01$ m s^{-1}, $k_s = 1.05$ W m^{-1}K^{-1} for glass spheres with $d = 3$ mm. The empirical constant D_t was found to be of the order of 10^{-2} [27]. However, since there is still a great deal of controversy on the thermal dispersion theory [28], this effect is considered with $D_t = 0.01$ for the purpose of a qualitative study. Since several non-Darcian flow effects will be taken into consideration, the following notations are used to stand for different effects throughout this study: BIU indicates Boundary, Inertia and Uniform porosity effects; nBnIU denotes no Boundary, no Inertia and Uniform porosity effects; BIV refers to Boundary, Inertia, and Variable porosity effects, and so on. It may be remarked that nBnIU is the Darcy flow case and has been reported recently by Hsieh *et al.* [21]. Results for this case from the previous study [21] and the present work have been compared and are found to be in excellent agreement.

Typical temperature profiles resulting from different flow models at selected values of n are depicted for pure free convection ($\chi = 0$) in Fig. 1, for mixed convection (e.g. at $\chi = 0.5$) in Fig. 2, and for pure forced convection ($\chi = 1$) in Fig. 3. In general, boundary and inertia effects are found to thicken the thermal boundary layer with a decrease in the wall temperature gradient. The basic cause of this behavior is that the flow inertia force and boundary viscous resistance retard the momentum transport, resulting in a reduction in heat transfer. When the boundary, inertia, and nonuniform porosity effects are considered simultaneously, the temperature gradient at wall can be either increased (associated with a decrease in the thermal boundary layer thickness) or decreased (associated with a thickened thermal boundary layer) as compared to the Darcy case, depending on the balance between these three effects. One also can see from these figures that, for a given flow model and at a fixed value of χ, a larger value of n gives rise to a larger wall temperature gradient associated with a decrease in the thermal boundary layer thickness. Thus, a higher value of n indicates a higher heat transfer rate from the wall.

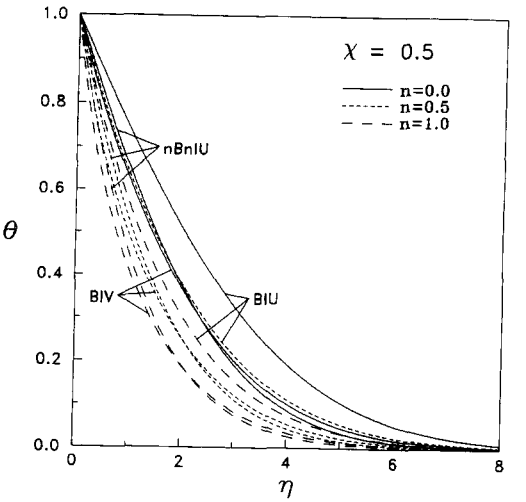

Fig. 2. Temperature profiles for $\chi = 0.5$.

Representative velocity profiles in terms of f' are illustrated for $\chi = 0.5$ in Fig. 4. It can be seen that the velocity profiles predicted by the non-Darcian models (BIV and BIU) differ significantly from those obtained by the Darcy's flow model (nBnIU) which allows a slip velocity at the solid boundary. We can conclude that boundary and inertia effects tend to decrease the velocity, while the nonuniform porosity effect causes an overshoot of velocity in the region very close to the wall. Since fluid inertia and viscous shear provide an additional pressure loss in the flow field, the velocity is reduced when boundary and iner-

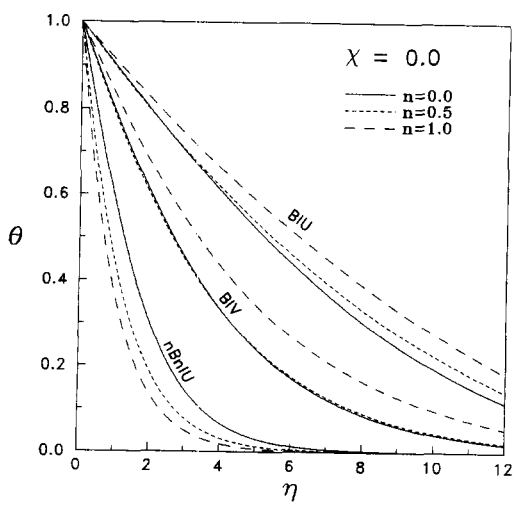

Fig. 1. Temperature profiles for $\chi = 0$.

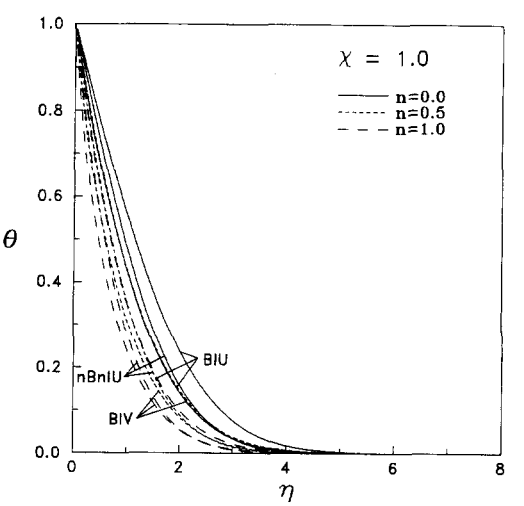

Fig. 3. Temperature profiles for $\chi = 1$.

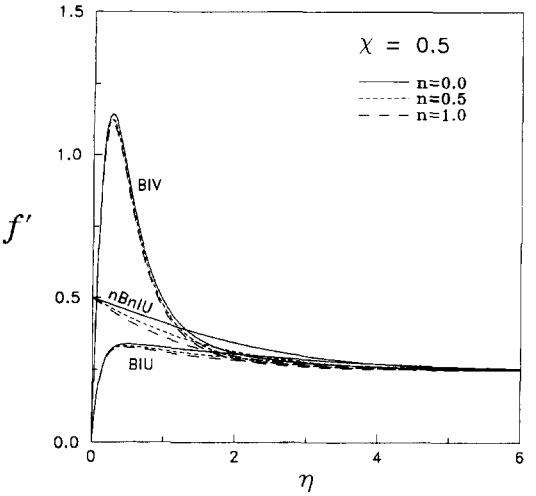

Fig. 4. Velocity profiles for $\chi = 0.5$.

tia effects (the BIU model) are considered. The channeling profile is readily understood from the fact that the porosity in the near-wall region is larger than that in the bulk region. Also, as n increases the momentum boundary layer thickness decreases for a specific flow model.

Figures 5 and 6 aim to identify the contribution of boundary, inertia, and variable porosity effects on the local Nusselt number in terms of $Nu_x(Pe_x^{0.5} + Ra_x^{0.5})^{-1}$. A comparison of local Nusselt number for the case of constant wall temperature ($n = 0$) is presented in Fig. 5. It is seen that when only the inertia effect is considered (the nBIU model), the decrease in the local Nusselt number is more pronounced at a smaller value of χ as compared to the Darcy's flow case (the nBnIU model). When boundary effect is also considered (the BIU model), the heat transfer rate is further reduced just to a slight degree as compared to the nBIU case. The present results also show that the inclusion of variable porosity effects (the nBIV and BIV models) tends to increase the heat transfer rate. It is noted that when different non-Darcian effects are considered simultaneously, the heat transfer rate can be either increased or decreased depending on the interactions among these effects under various conditions. This is clearly shown in Figs. 5 and 6. Figure 6 shows the predicted local Nusselt numbers for different values of n. It is clear from this figure that, for a given value of n, the heat transfer rate decreases when the Brinkman friction term and the Forchheimer inertia term are included (the BIU model). As mentioned above, the flow-channeling effect tends to augment the heat transfer from the wall. Also, when all three effects are taken into account (the BIV model), the competition among these non-Darcian mechanisms determines whether the heat transfer will be enhanced or reduced. For the Darcy flow case, it is seen that the local Nusselt number decreases at first, reaches a minimum value, and then increases with increasing χ. This can be made clear from the nature of the $Nu_x(Pe_x^{0.5} + Ra_x^{0.5})^{-1}$ vs χ plot, which does not imply that the actual Nu_x value for mixed convection is smaller than that for pure forced convection or pure free convection. In fact, the predicted value of local Nusselt number for mixed convection is higher than that for pure forced convection and pure free convection, as was demonstrated in [21]. Unlike the Darcy flow behavior, the local Nusselt number variations with χ in non-Darcian flow models (BIU and BIV) exhibit a continuous increase with increasing χ. Also, for a given flow model, the Nusselt number increases as n increases.

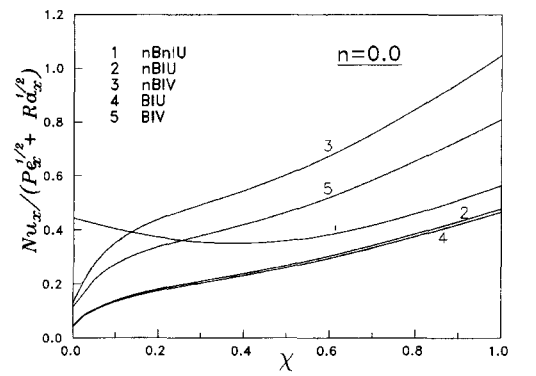

Fig. 5. Comparison of local Nusselt number for $n = 0$.

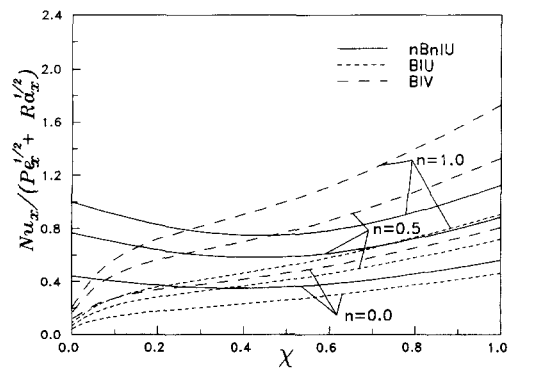

Fig. 6. Local Nusselt number at selected values of n.

The last non-Darcian effect to be examined in the analysis is the thermal dispersion, which is expected to be more noticeable as the flow inertia becomes prevalent. Effects of thermal dispersion on the local Nusselt number are presented for an isothermal vertical plate ($n = 0$) in Fig. 7 and for a nonisothermal plate with $n = 1$ in Fig. 8. It can be summarized from these two figures that the local Nusselt number increases tremendously when the thermal dispersion effect is taken into account. This great enhancement in heat transfer can be attributed to the dispersive transport which brings about a better mixing of convective fluid within the pores.

CONCLUDING REMARKS

The foregoing study has been conducted to demonstrate the importance of non-Darcy effects on mixed

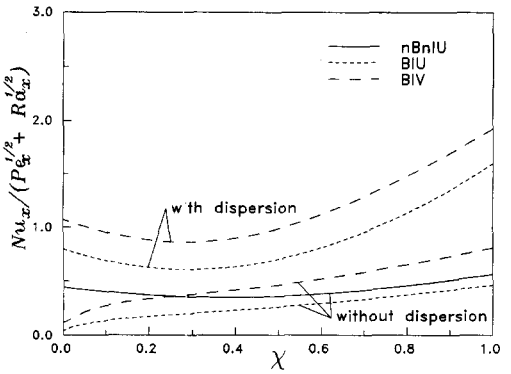

Fig. 7. Effects of thermal dispersion on local Nusselt number for $n = 0$.

convection along a vertical flat plate embedded in a porous medium for the case of power-law variation in wall temperature. Effects of flow inertia, boundary friction force, and nonuniform porosity are taken into account in the momentum equation. Owing to the near-wall porosity variation, it is expected that the thermal conductivity will vary across the porous medium. Effects of variable stagnant thermal conductivity and transverse thermal dispersion are taken into consideration in the energy equation. The local Nusselt numbers are presented for the entire mixed convection regime, ranging from pure forced convection ($\chi = 1$) to pure free convection ($\chi = 0$). It has been found that inclusion of non-Darcian effects significantly alters the flow and heat transfer characteristics from those predicted by the traditional Darcy's model. Effects of flow inertia and boundary friction force with the no-slip boundary condition tend to reduce the velocity and heat transfer, while the flow-channeling effect, caused by the near-wall porosity variation, enhances the momentum and thermal transports in the boundary layer. Whether the heat transfer will be increased or decreased as compared to the Darcy flow depends on the competition between these three effects. Finally, the thermal dispersion effect is found to increase considerably the local Nusselt number.

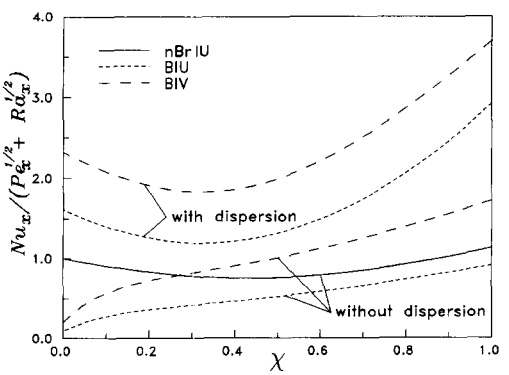

Fig. 8. Effects of thermal dispersion on local Nusselt number for $n = 1$.

Acknowledgements—Financial support for this study provided by the National Science Council of Republic of China through grant no. NSC 83-0117-C-150-031-E is greatly appreciated.

REFERENCES

1. W. J. Minkowycz and P. Cheng, Free convection about a vertical cylinder embedded in a porous medium, *Int. J. Heat Mass Transfer* **19,** 805–813 (1976).
2. P. Cheng and W. J. Minkowycz, Free convection about a vertical flat plate embedded in a porous medium with application to heat transfer from a dike, *J. Geophys. Res.* **82,** 2040–2044 (1977).
3. A. Nakayama and H. Koyama, A general similarity transformation for combined free and forced-convection flows within a fluid-saturated porous medium, *J. Heat Transfer* **28,** 1041–1045 (1987).
4. H. M. Badr and I. Pop, Combined convection from an isothermal horizontal rod buried in a porous medium, *Int. J. Heat Mass Transfer* **31,** 2527–2541 (1988).
5. J. T. Hong, Y. Yamada and C. L. Tien, Effects of non-Darcian and nonuniform porosity on vertical-plate natural convection in porous medium, *J. Heat Transfer* **109,** 356–362 (1987).
6. K. Vafai and C. L. Tien, Boundary and inertia effects on flow and heat transfer in porous media, *Int. J. Heat Mass Transfer* **24,** 195–203 (1981).
7. P. Ranganathan and R. Viskanta, Mixed convection boundary layer flow along a vertical porous medium, *Numer. Heat Transfer* **7,** 305–317 (1984).
8. G. Lauriat and V. Prasad, Natural convection in a vertical porous cavity: a numerical study for Brinkman–extended Darcy formulation, *J. Heat Transfer* **109,** 688–696 (1987).
9. G. Lauriat and V. Prasad, Non-Darcian effects on natural convection in a vertical porous enclosure, *Int. J. Heat Mass Transfer* **32,** 2135–2148 (1989).
10. C. Y. Choi and F. A. Kulacki, Non-Darcian effects on mixed convection: a vertical packed-sphere annulus, *J. Heat Transfer* **115,** 506–510 (1993).
11. R. F. Benenati and C. B. Brosilow, Void fraction distribution in beds of spheres, *A.I.Ch.E. J* **8,** 359–361 (1962).
12. D. Vortmeyer and J. Schuster, Evaluation of steady flow profiles in rectangular and circular packed beds, *Chem. Engng Sci.* **38,** 1691–1699 (1983).
13. K. Vafai, Convective flow and heat transfer in variable-porosity media, *J. Fluid Mech.* **147,** 233–259 (1984).
14. E. David, G. Lauriat and P. Cheng, A numerical solution of variable porosity effects on natural convection in a packed-sphere cavity, *J. Heat Transfer* **113,** 391–399 (1991).
15. P. Cheng, Thermal dispersion effects in non-Darcian convective flows in a saturated porous medium, *Lett. Heat Mass Transfer* **8,** 267–270 (1981).
16. O. A. Plumb, The effect of thermal dispersion on heat transfer in packed bed boundary layers, *Proceedings of the ASME/JSME Joint Thermal Conference*, Vol. 2, pp. 17–21 (1983).
17. A. Yucel, The influence of injection or withdrawal of fluid on free convection about a vertical cylinder in a porous medium, *Numer. Heat Transfer* **7,** 483–493 (1984).
18. W. J. Minkowycz, P. Cheng and C. H. Chang, Mixed convection about a nonisothermal cylinder and sphere in a porous medium, *Numer. Heat Transfer* **8,** 349–359 (1985).
19. T. Cebeci and P. Bradshaw, *Physical and Computational Aspects of Convective Heat Transfer*. Springer, New York (1984).
20. T. K. Aldoss, T. S. Chen and B. F. Armaly, Non-similarity solutions for mixed convection from hori-

zontal surfaces in a porous medium-variable wall temperature, *Int. J. Heat Mass Transfer* **36,** 471–477 (1993).
21. J. C. Hsieh, T. S. Chen and B. F. Armaly, Mixed convection along a nonisothermal vertical flat plate embedded in a porous medium : the entire regime, *Int. J. Heat Mass Transfer* **36,** 1819–1825 (1993).
22. L. H. S. Roblee, R. M. Baird and J. W. Tierney, Radial porosity variations in packed beds, *A.I.Ch.E.J* **4,** 460–464 (1958).
23. C. H. Chen and J. S. Chiou, Conjugate free convection heat transfer analysis of a vertical plate fin embedded in non-Darcian porous media, *Int. J. Engng Sci.* **32,** 1703–1716 (1994).
24. M. L. Hunt and C. L. Tien, Non-Darcian convection in cylindrical packed beds, *J. Heat Transfer* **110,** 378–384 (1988).
25. S. Ergun, Fluid flow through packed columns, *Chem. Engng Prog.* **48,** 89–94 (1952).
26. P. Zehner and E. U. Schluender, Waermeleitfahigkeit von schuettungen bei massigen temperaturen, *Chemie Ingr Tech.* **42,** 933–941 (1970).
27. C. T. Hsu and P. Cheng, Closure schemes of the macroscopic energy equation for convective heat transfer in porous media, *Int. Commun. Heat Mass Transfer* **15,** 689–703 (1988).
28. M. Kaviany, *Principles of Heat Transfer in Porous Media.* Springer, New York (1991).